

Contents lists available at [SciVerse ScienceDirect](http://www.sciencedirect.com)

Solid-State Electronics

journal homepage: www.elsevier.com/locate/sse

Improvement of metal gate/high-*k* dielectric CMOSFETs characteristics by neutral beam etching of metal gate

K.S. Min^{a,d,e}, C. Park^e, C.Y. Kang^e, C.S. Park^e, B.J. Park^f, Y.W. Kim^b, B.H. Lee^c, Jack C. Lee^d, G. Bersuker^e, P. Kirsch^e, R. Jammy^e, G.Y. Yeom^{a,*}

^a Department of Advanced Materials Science and Engineering, Sungkyunkwan University, Suwon, Gyeonggi-do 440-746, Republic of Korea

^b Department of Materials Science and Engineering, Seoul National University, Seoul 151-744, Republic of Korea

^c Department of Nanobio Materials and Electronics, Gwangju Institute of Science and Technology, Gwangju 500-712, Republic of Korea

^d Microelectronics Research Center, Department of Electrical and Computer Engineering, The University of Texas, Austin, TX 78758, USA

^e SEMATECH, Austin, TX 78741, USA

^f Process Development Team, Semiconductor R&D center, Samsung Electronics, San #16 Banwol-Dong, Hwasung-City, Gyeonggi-Do 445-701, Republic of Korea

ARTICLE INFO

Article history:

Received 11 October 2011

Received in revised form 15 June 2012

Accepted 24 July 2012

Available online xxx

Communicated by: Associate Editor.

S. Cristoloveanu

Keywords:

Neutral beam etching

Metal gate

Complementary metal–oxide–semiconductor field effect transistors (CMOSFETs)

ABSTRACT

For the metal gate patterning of metal gate/high-*k* dielectric complementary metal–oxide–semiconductor field effect transistors (CMOSFETs), plasma induced damage (PID) was identified during the etching by a conventional reactive ion etching (RIE) and, a neutral beam etching (NBE) technique. NBE uses reactive radical beam instead of reactive ions for RIE. Improved device characteristics such as the mobility, the transconductance, subthreshold slope, and drain current could be observed. Particularly, the application of the NBE to PMOSFET was more effective than that to NMOSFET. This improvement was related to the decreased interface trap density at the gate dielectric of CMOSFETs.

© 2012 Published by Elsevier Ltd.

1. Introduction

As the critical dimension (CD) of the metal–oxide–semiconductor field effect transistor (MOSFET) is scaled down to 45 nm node and below, high dielectric constant materials become an attractive alternative to SiO₂. However, the poly-Si with high-*k* dielectric shows a limitation in the work function tunability at the poly-Si/M_eO_x interfaces. This limits the threshold voltage control in complementary MOSFETs (CMOSFETs), particularly in *p*-channel MOSFET (PMOSFET). Therefore, a metal gate with high-*k* dielectric has been considered [1].

For the metal gate patterning, reactive ion etching (RIE) has been generally used to etch anisotropically for the accurate CD control. Previous works have shown that using HBr/Cl₂ gas, high TiN etch rate was obtained in addition to the highly anisotropic etch profile of poly-Si/TiN/HfO₂/Si in the inductively coupled plasmas (ICPs) [2], and CD was controlled not exceeding 2 nm and profiles close to vertical were achieved in sub-45 nm TaN/HfAlO/Si [3].

However, during these metal gate etching, plasma induced damage (PID) can be generated and it can degrade the electric characteristics of metal gate/high-*k* dielectric CMOSFETs [4,5].

PID during the etching of a gate structure by RIE consists of plasma induced charging damage (PICD) and plasma induced edge damage (PIED) [6]. PICD is mainly caused by the high-field stressing of thin gate oxides during plasma processing. A local imbalance of the ion current density from the plasma to the substrate or the differences in the etch endpoint during the gate etching induces plasma induced charging current (PICC) across the gate oxide. And, a high stress voltage developed by the PICC across the gate oxide results in forming interface traps near the gate oxide [7]. In the case of poly-Si/SiO₂/Si, PICD can be formed during the poly-Si etching. However, in the case of poly-Si/TiN/HfO₂/Si, it can be formed during the metal gate etching because the presence of a metal gate can prevent local imbalanced ions during poly-Si etching. It is known that, in poly-Si/aggressively scaled SiO₂ CMOSFETs, PICD is no longer a problem because of the low stress voltage for a given PICC [8]. However, given the higher physical thickness of high-*k* dielectrics compared to SiO₂, the problem could be reintroduced due to higher stress voltage. [9,10].

Neutral beam etching (NBE) has been introduced previously by many researchers to remove possible PID during the etching of

* Corresponding author at: Department of Advanced Materials Science and Engineering, Sungkyunkwan University, Suwon, Gyeonggi-do 440-746, Republic of Korea. Tel.: +82 31 299 6560; fax: +82 31 299 6565.

E-mail address: gyyeom@skku.edu (G.Y. Yeom).

semiconductor devices. The neutralized reactive radical beam was generally formed by neutralizing the reactive ions using various methods such as neutralization by the reflection of ions on the low angle reflector, neutralizing reflection on the sidewall of the grid hole during the extraction of ions from a plasma source, etc. [11–15]. Previously, using CHARM[®] 2 monitoring wafers after etching no significant change in positive charging, negative charging and UV damage was observed compared to RIE. NBE has been applied to a MOS capacitor structure and showed the possibility of removal of PICD [11] and also other applications such as (AAO) [12], MRAM, recently [13]. However, the effect of NBE on PICD in metal gate/high-*k* dielectric CMOSFETs has not been systematically studied.

In this article, a NBE has been applied to the etching of CMOSFET metal gate composed of poly-Si/TiN/HfO₂/SiO₂/Si after the poly-Si etching and the effect of the metal gate etching using NBE on the electrical characteristics of CMOSFETs was compared with those etched using conventional RIE.

2. Experimental

Metal gate/high-*k* dielectric CMOSFETs with the gate width (*W*) of 10 μm and the gate length (*L*) of 1 μm were fabricated using a standard complementary MOS process except for TiN metal gate etching. The gate stacks include 1000 Å poly-Si/100 Å TiN/30 Å HfO₂/interfacial 10 Å SiO₂ on Si substrate. TiN metal gate was etched by an optimized RIE or NBE process. RIE was carried out using rf-biased Cl₂-based inductively coupled plasma (ICP). The NBE was carried out for 2 min 30 s using a low angle reflected HBr/Cl₂ NBE system composed of a three-grid ICP ion source installed with a low angle reflector in front of the ICP ion source for the neutralization of reactive ion beam (>90% neutralization efficiency). The details of the NBE system can be found [11]. After the metal gate etching with the RIE or the NBE, the high-*k* dielectric was removed with a HF-based wet etching after slight Ar⁺ ion physical bombardment by a RIE system.

Equivalent oxide thickness (EOT) was extracted from the measured capacitance–voltage (*C–V*) curves on a MOS capacitor (MOSCAP) with an area of 200 μm² using North Carolina State University (NCSU) CVC model and the EOT was calculated to be about 1.2 nm for the etching of metal gate using both RIE and NBE indicating no variation of EOT after the metal gate etching. Transmission electron microscope (TEM) of the CMOSFET gate after the NBE of TiN gate metal is shown in Fig. 1. As shown in the figure, a similar slightly tapered etch profile could be obtained after the TiN metal gate etched by the RIE. The etch profiles in both cases ((a) RIE and (b) NBE) is similar.

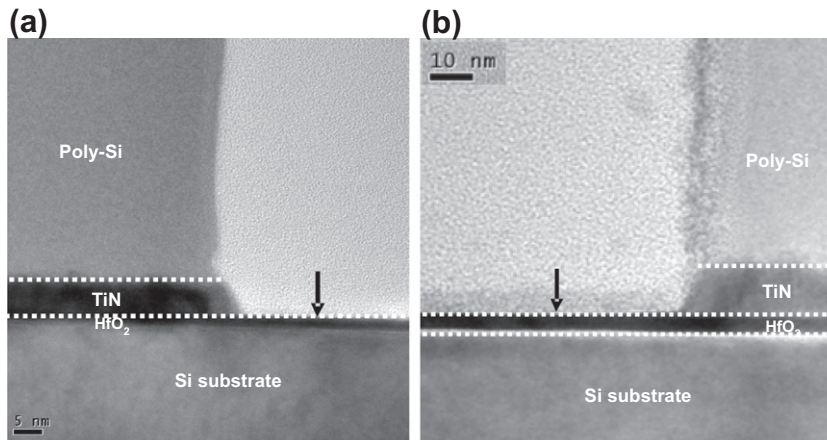


Fig. 1. Cross-sectional TEM images of the gate stacks after (a) RIE and (b) NBE.

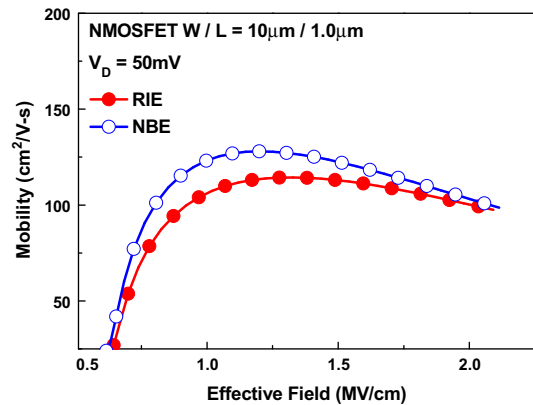


Fig. 2. Effective mobility for NMOSFET with *W/L* = 10 μm/1 μm after RIE and NBE.

3. Results and discussion

PICD affects the interface state in the gate oxide of the CMOSFET. The effective field electron mobility is known to be more sensitive to the interface state than other MOS parameters [16]. Fig. 2 shows the effective field electron mobility measured as a function of effective field for the NMOSFETs with *W/L* = 10 μm/1 μm after RIE and NBE. The mobility was extracted using NCSU mob2d model [17]. As shown in the figure, the maximum effective field electron mobility for NBE (127.2 cm²/V s) was 10.1% higher than that for RIE (114.4 cm²/V s). This is attributed to the low PICD inducing interface states at the gate oxide. Note that the effective field electron mobility of the NMOSFET after RIE is consistent with the previous report [1].

MOS parameters (transconductance (*G_m*), threshold voltage (*V_{th}*), subthreshold swing (*SS*), drain current (*I_D*) and gate leakage current (*I_G*) are also sensitive to PICD. This PICD has the polarity depending on a gate dielectric. In the case of SiO₂, PICD has the different polarity, which leads to shift *V_T* of PMOSFET in the opposite direction to NMOSFET. However, in another case of a high-*k* dielectric (HfO₂), *V_T* is moved to the same direction, positively in both NMOSFET and PMOSFET [18]. The typical method of PICD estimation is to detect the degradation of the MOS parameters directly. Therefore, MOS parameters were extracted from the *I_D–V_G* measurement. Fig. 3 shows the *I_D–V_G* measured for (a) NMOSFET and (b) PMOSFET after the metal gate etching by RIE and NBE. As shown in Fig. 3a, in the case of NMOSFET, the normalized maximum *G_m* for NBE was 9.3% higher than that for RIE while the *SS* for NBE was 6.5% lower than that of RIE. The *SS* is related to the interface trap. Therefore, *D_{it}* in NBE is could be lower than that of

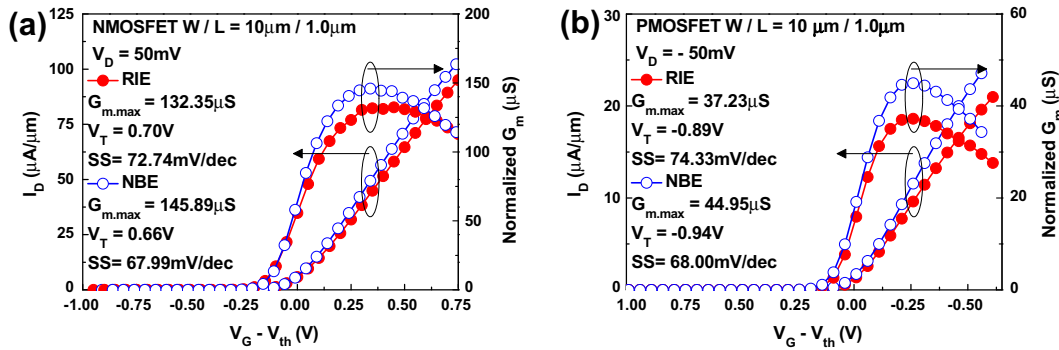


Fig. 3. I_D - V_G measured for the CMOSFET with $W/L = 10 \mu\text{m}/1 \mu\text{m}$ after RIE and NBE.

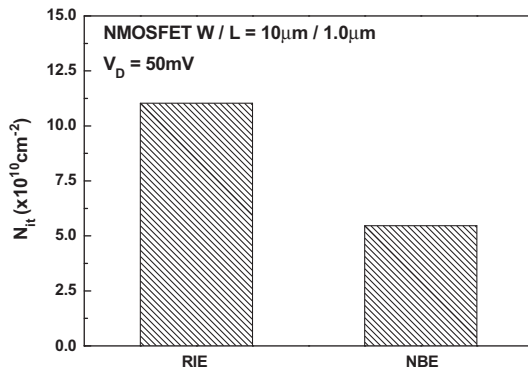


Fig. 4. MOS parameters (gate leakage current (I_G)) degradation for the reference (without the antenna structure) and two main types of antenna structure: area antenna and perimeter antenna for the NMOSFETs with $W/L = 10 \mu\text{m}/1 \mu\text{m}$ after RIE and NBE.

RIE. In addition, the increase of 8.9% in I_D , which is attributed to the improved effective field electron mobility, could be observed for NBE. In the case of PMOSFET, the normalized maximum G_m and for NBE was 17.2% higher than that for RIE, and the SS for NBE was 8.5% lower than that of RIE, and I_D was 16.9% higher for NBE. Therefore, MOS parameters were generally improved after the metal gate etching by NBE due to the decreased PICD and, the MOS parameters of PMOSFET were improved more than those of NMOSFET because PICD is more sensitive to PMOSFET than NMOSFET due to easier electron injection causing the interface state for n -type substrate than p -type Si substrate [19].

The degradation of the gate oxide could be observed by measuring the interface state density (N_{it}) using charge pumping method operated at 1 MHz for the characterization of the N_{it} [6]. Fig. 4 shows the N_{it} measured on the NMOSFET devices after the RIE and NBE. As shown in the figure, the N_{it} after the NBE ($5.4 \times 10^{10} \text{cm}^{-2}$) was 52.2% lower than that after RIE ($11.3 \times 10^{10} \text{cm}^{-2}$). The N_{it} observed after the NBE might be originated from the growth of high- k dielectric on silicon by ALD, but RIE caused PICD across the high- k dielectric, which resulted in the increase of N_{it} . Note that the N_{it} of the NMOSFET after RIE is consistent with the previous report [1]. Therefore, the smaller N_{it} for NBE implies that NBE produces less gate oxide degradation due to the lack of the PICD inducing interface state compared to RIE. This result is consistent with the improvement of the mobility and the MOS parameters observed after the metal gate etching using the NBE instead of RIE as described earlier.

Additionally, SEMATECH SPIDER, which has previously been used to evaluate the origins of PICD was prepared to investigate the source of the differences in MOS parameters after NBE and RIE. These modules in SPIDER have structures without or with

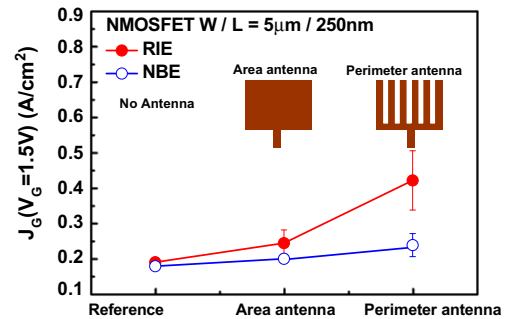


Fig. 5. N_{it} extracted using charge pumping method operated at 1 MHz.

antenna connected to the gate. The antenna area ratio (AR) is defined as the area ratio of antenna connected to the gate over the thick field oxide to the gate over the thin oxide. It enables a high sensitivity for PICD introduced by plasma etching. Each antenna module is sensitive to a particular plasma etching step. Therefore, the polysilicon/TiN gate antenna module, which is sensitive to PICD during gate etching step was used. The antenna module has two main types of antennas: area antenna (AR = 23 K) and perimeter antenna (AR = 23 K). Fig. 5 shows MOS parameters (gate leakage current (I_G) at $V_G = -1.5\text{V}$) degradation for the reference (without the antenna structure) and the gate with two main types of antenna structure: area antenna and perimeter antenna for the NMOSFETs with $W/L = 10 \mu\text{m}/1 \mu\text{m}$ of 250 nm after RIE and NBE. In the case of RIE, I_G degradation was observed for the gate with the antenna structure and was also increased with the increase of the sidewall exposed area of the antenna structure. On the other hand, in the case of NBE, less change of I_G was observed for all both (with/without) the antenna modules. Therefore, the degradation of the MOS parameters in Fig. 3 was attributed to PICD.

4. Conclusions

This study demonstrates that NBE process is very promising to metal gate etching after poly-Si etching in metal gate/high- k dielectric CMOSFETs which is capable of lower PICD than RIE. Further studies on the effect of NBE on high-mobility transistor seem to be needed because PICD would be more critical to high-mobility semiconductors such as III-V compound semiconductors due to more electron injection properties leading to PICD across the gate oxide from the substrate.

Acknowledgments

This work was supported by the National Research Foundation of Korea Grant funded by the Korean Government (MEST)

(NRF-2010-M1AWA001-2010-0026248) and was financially supported by the Ministry of Knowledge Economy (MKE) and Korea Institute for Advancement of Technology (KIAT) through the Workforce Development Program in Strategic Technology.

References

- [1] Hobbs CC, Fonseca LRC, Knizhnik A, Dhandapani V, Samavedam SB, Taylor WJ, et al. *IEEE Trans Electron Dev* 2004;51(6):971–7.
- [2] Le Gouil A, Joubert O, Cunge G, Chevolleau T, Vallier L, Chenevier B, et al. *J Vac Sci Technol B* 2007;25:3.
- [3] Bliznetsov VN, Bera LK, Soo HY, Balasubramanian N, Kumar R, Qiang Lo G, et al. *IEEE Trans Semicond Manuf* 2007;49:1.
- [4] Tzeng PJ, Chang YY, Chang-Liao KS. *IEEE Electron Dev Lett* 2001;22:11.
- [5] Hussain MM, Song SC, Barnett J, Kang CY, Gebara G, Sassman B, et al. *IEEE Electron Dev Lett* 2006;27:12.
- [6] Chen SJ, Chung SSS, Lin HC. *Jpn J Appl Phys* 2002;41.
- [7] Cheung KP. In: *Proc int conf solid-state & integrated circuit technol*; 2001.
- [8] Park D, Hu C. *IEEE Electron Dev Lett* 1998;19:1.
- [9] Fang S, Murakawa S, Mcvittie JP. In: *Tech dig – int electron devices meet*; 1992. p. 61.
- [10] Min KS, Kang CY, Yoo OS, Park BJ, Kin SW, Young CD, et al. In: *Proc of int rel phys symp*; 2008. p. 723.
- [11] Park BJ, Kim SW, Kang SK, Min KS, Park SD, Kyung SJ, et al. *J Phys D: Appl Phys* 2008;41.
- [12] Yeon JK, Lim WS, Park JB, Kwon NY, Kim SI, Min KS, et al. *J Electrochem Soc* 2011;158.
- [13] Kang S K, Jeon MH, Park JY, Yeom GY, Jhon MS, Koo BW, et al. *J Electrochem Soc* 2011.
- [14] Samukawa S, Sakamoto K, Ichiki K. *J Vac Sci Technol B* 2002;20:1566.
- [15] Ranjan A, Donnelly VM, Economou DJ. *J Vac Sci Technol A* 2006;24:5.
- [16] Vogel EM, Ahmed KZ, Hornung B, Henson WK, McLarty PK, Lucovsky G, et al. *IEEE Trans Electron Dev* 1998;45.
- [17] Islam AE, Matheta VD, Das H, Mahapatra S, Alam MA. In: *Proc IEEE IRPS*; 2008. p. 87.
- [18] Young CD, Bersuker G, Zhu F, Matthews K, Choi R, Song SC, et al. In: *Proc of int rel phys symp*; 2007. p. 67.
- [19] Chen CC, Lin HC, Chang CY, Liang MS, Chien CH, Hsien SK, et al. *IEEE Electron Dev Lett* 2000;47:7.